Electronic Supplementary Material (ESI) for Nanoscale.
This journal is @ The Royal Society of Chemistry 2020

Electronic Supplementary Information

Large piezoelectric and thermal expansion coefficients with negative Poisson's ratio in strain-modulated Tellurene†

Parrydeep Kaur Sachdeva[abc], Shuchi Gupta[b] and Chandan Bera*[a]

[a] Institute of Nano Science and Technology, Knowledge City, Sector-81, S.A.S Nagar, Mohali, Punjab 140306, India
[b] University Institute of Engineering and Technology, Panjab University, Sector-25, Chandigarh-160014
[c] Department of Physics, Panjab University, Sector-14, Chandigarh 160014, India

E-mail: chandan@inst.ac.in

I. PIEZOELECTRIC EFFECT IN BULK TELLURIUM

The bulk Tellurium falls into the category of non-centrosymmetric materials. The optimized lattice parameters are a = 4.51 Å, b = 4.51 Å and c = 5.96 Å. It has trigonal lattice with space group $P3_121$ (152) and this lattice has the piezoelectric tensor of the form:

$$e_{ij} = \begin{pmatrix} e_{11} & -e_{11} & 0 & 0 & 0 & -e_{16} \\ 0 & 0 & 0 & 0 & e_{16} & 0 \\ 0 & 0 & 0 & 0 & 0 & 0 \end{pmatrix} \quad (1)$$

Bulk Te has only two independent piezoelectric elements. Therefore, we obtained these two stress piezoelectric coefficients in bulk system as:
$e_{11} = 1.19\ C/m^2$ and $e_{16} = 0.30\ C/m^2$.
These coefficients indicate that bulk Tellurium exhibits very small piezoelectricity.

II. ENERGY VS STRAIN CURVES

We have performed DFT calculations to determine the structural energies of β and β'-Tellurene. We relaxed all the structures that were strained with compressive and tensile strain along the armchair and zigzag directions from -10% to +10%. Figure S1 shows the variation in the lateral lattice parameter upon straining the axis of β-Te. Compressive strain in a (or b) axis leads to tensile strain in b (or a) parameter. Similarly, stretching in a (or b) axis leads to shrinking in b (or a) parameter. We determined the energies for the deformed structures of β'-Te too (Fig. S2). Its behavior is similar to that of β-Te for applied strain in armchair direction. However, for the applied strain in zigzag direction (b-axis), it is observed that 'a' lattice constant seems to be non-varying under tensile strain in the b-axis because of the very small increments. This increment is visible in the Poisson's ratio plots clearly (Fig. 2). It can be interpreted that tensile strain in zigzag direction does not bring about major changes in armchair direction due to chair like structure of Tellurene.

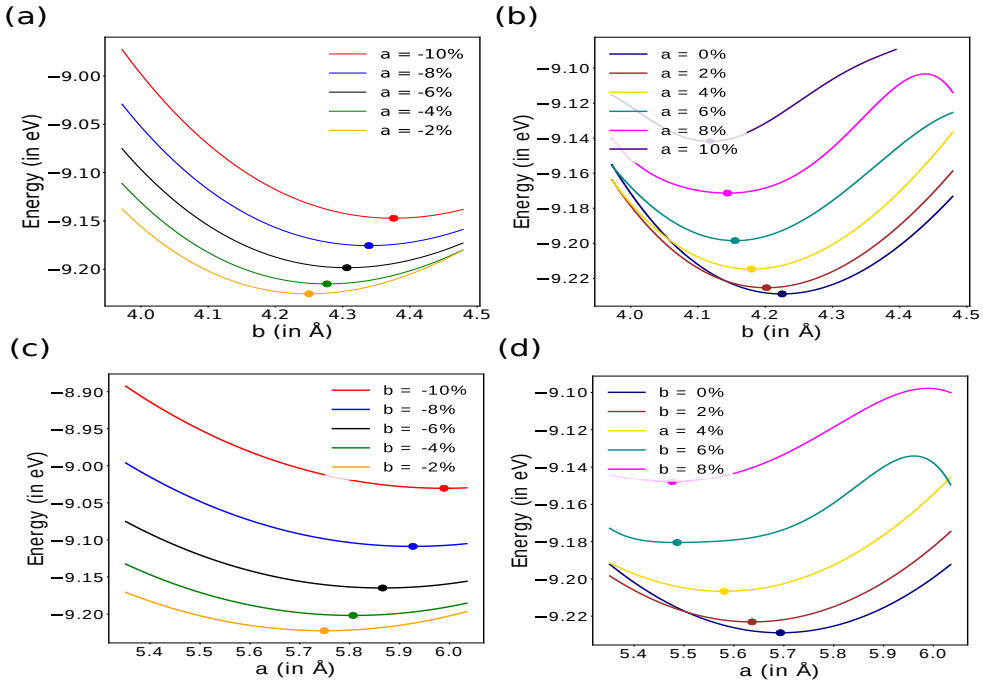

Figure S1. Energy variation for β-Tellurene monolayer with applied strain in the armchair and zigzag directions.

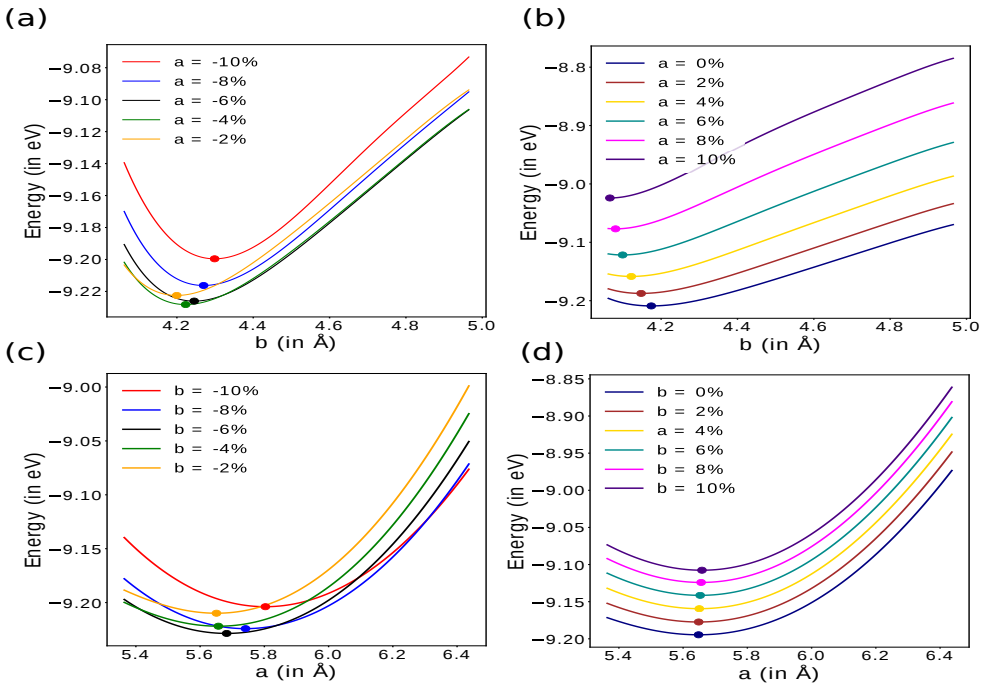

Figure S2. Energy variation for $\beta^{'}$-Tellurene monolayer with applied strain in the armchair and zigzag directions.

III. POISSON'S RATIO

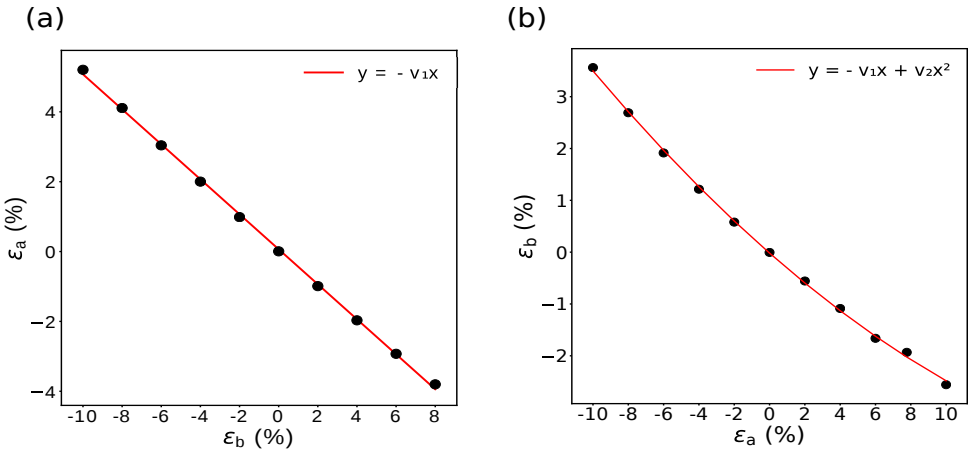

Figure S3. Poisson's ratio as a function of uniaxial deformation of β-Te: (a) ϵ_a vs ϵ_b. (b) ϵ_b vs ϵ_a.

Poisson's ratio is the ratio of response strain to the applied strain. Strain is given by

$$\epsilon = (l - l_0)/l_0 \tag{2}$$

where l refers to the deformed length and l_0 is the original length. The linear Poisson's ratio (v_1) for β-Te based on Fig. S3 is found to be 0.49 and 0.29 along the zigzag and armchair directions fitted to the linear line and a second order polynomial, respectively.

IV. EVOLUTION OF STRUCTURE UNDER STRAIN

The single layer $\beta^{'}$-Tellurene is a puckered structure that consists of the non-planar chair-like six-membered ring which redistributes the mechanical strain in such a way that the positive strain along the b-axis leads to very small strain along a-direction. Also, due to the puckered nature of Tellurene, it is more likely to be easily stretchable under large mechanical strains. The evolution of local structure or in other words, the movement of atoms of Tellurene monolayer under the uniaxial deformation helps in understanding the NPR behavior. We particularly present the phenomenon for redistribution of the applied tensile strain of 10% along b-direction as shown in Fig 2.

Here, the structure is stretched in the b-direction which increases the bond length $r_{51}(=r_{52})$ and ϕ_{157} and decreases ϕ_{152} as tabulated in Table S1. Due to the outward increased motion of atoms 1 and 2, there is an inward motion of atoms 7 and 8 towards atom 5 and this decreases $r_{75}(=r_{85})$. It has been observed that atom 5 moves a bit outward. The atoms 3,4,6,9 and 10 also shift in a similar way. To combat this expansion in b-direction as well as in a-direction, atoms 2,3 and 8,9 move towards each other and this decreases the effective thickness (d) and increases ϕ_{758} of the non-planar sheet. So, this shows that stretching of chair-like ring in the zigzag direction reduces its non-planarity. We can say that with the increased strain, the structure can lose its non-planarity. This explains the in-plane NPR behavior. This also points towards the out-of-plane PPR behaviour which is responsible for compensating all the expansion happening in the structure.

TABLE S1. Bond lengths (r), bond angles (ϕ) and effective thickness (d) of $\beta^{'}$-Tellurene under uniaxial deformation in the zigzag direction. The units of r and ϕ are Å and degrees.

Monolayer	r_{51}	r_{75}	ϕ_{152}	ϕ_{157}	ϕ_{758}	**d**
uniaxial strain along zigzag(0%)	3.39	2.85	78.39	91.98	97.62	4.07
uniaxial strain along zigzag(10%)	3.83	2.78	67.88	95.91	100.29	4.02

V. PIEZOELECTRICITY IN β-TE

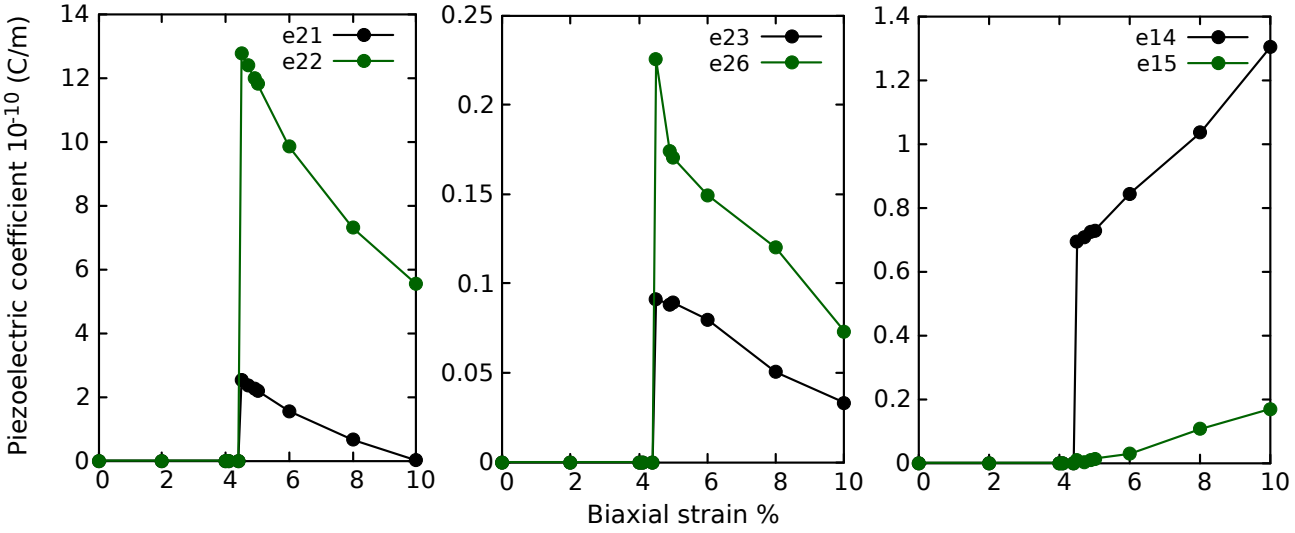

Figure S4. (a)-(c) Variation in Piezoelectric stress coefficients of β-Te as a function of biaxial strain. Variation of all the six non-zero independent tensors is shown.

β-Te has inversion symmetry and hence due to structural centrosymmetry, it shows no piezoelectric effect. The application of external strain disturbs its symmetry and changes into P2 non-centrosymmetric structure. This phase transition results in piezoelectricity. Figure. S3 shows the phase transition, particularly at 4.5% tensile biaxial strain. The highest in-plane coefficient obtained at this strain is 12.76 $\times$ 10^{-10} C/m. This value is smaller as observed in $\beta^{'}$-Te, although it is larger than the MoS_2. Therefore, $\beta^{'}$-Te exhibits larger piezoelectricity than β-Te. The effect of uniaxial strain is also determined. β-Te is centrosymmetric in the whole strain range of +10% to -10% uniaxial strain in the armchair and zigzag directions. Therefore, no piezoelectricity is observed under the applied uniaxial strain.

VI. BORN-EFFECTIVE CHARGES

TABLE S2. Diagonal elements of the Born effective charges of $\beta^{'}$-Te for unstrained monolayer and under biaxial and uniaxial strains are calculated using DFPT. Here, Te5, Te2 and Te3 represent the Tellurene atoms as numbered in Fig. 1(a). The unit cell contains these three Te atoms.

Monolayer	$\boldsymbol{Te5_{xx}}$	$\boldsymbol{Te5_{yy}}$	$\boldsymbol{Te5_{zz}}$	$\boldsymbol{Te2_{xx}}$	$\boldsymbol{Te2_{yy}}$	$\boldsymbol{Te2_{zz}}$	$\boldsymbol{Te3_{xx}}$	$\boldsymbol{Te3_{yy}}$	$\boldsymbol{Te3_{zz}}$
unstrained	1.22	3.86	0	-0.61	-1.93	0	-0.61	-1.93	0
biaxial strain (-5.5%)	1.87	7.92	0.04	-0.94	-3.97	-0.02	-0.94	-3.97	-0.02
uniaxial strain along zigzag(-4.9%)	1.81	7.44	0.03	-0.90	-3.73	-0.01	-0.90	-3.73	-0.01

VII. ELECTRONIC BAND STRUCTURE

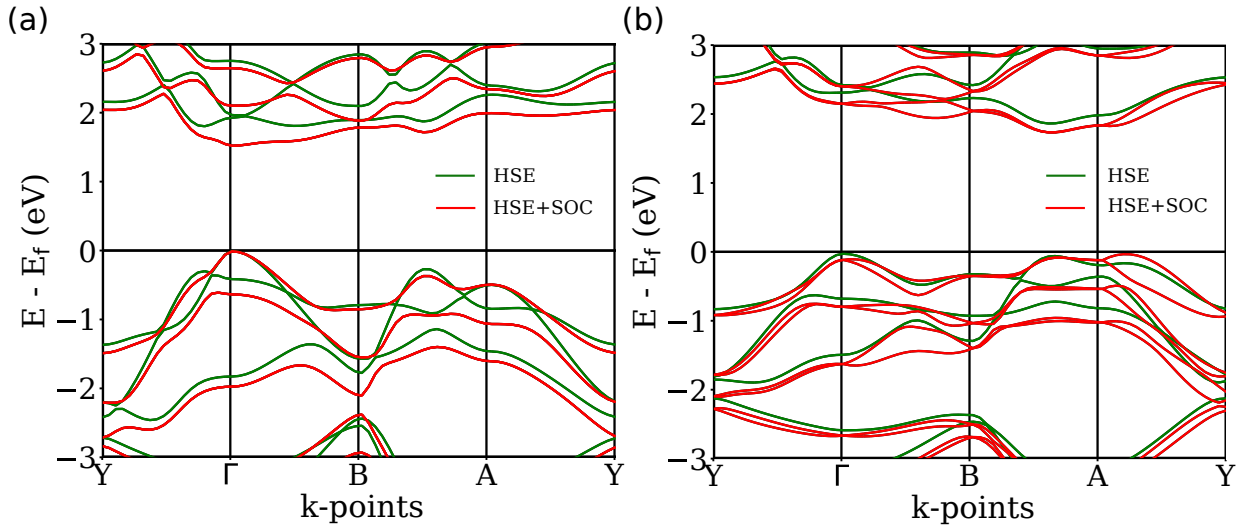

Figure S5. Band structures of (a) β-Te and (b) $\beta^{'}$-Te using HSE06 with and without spin-orbit coupling.

TABLE S3. Band gaps of β and $\beta^{'}$-Te using functionals HSE with and without the inclusion of spin-orbit coupling. D and I represent the direct and indirect band gaps, respectively.

Monolayer	**Functional**	**Band gap (eV)**
β-Te	HSE	1.81 (I)
	HSE+SOC	1.48 (D)
$\beta^{'}$-Te	HSE	1.89 (I)
	HSE+SOC	1.74 (I)

VIII. ELASTIC CONSTANTS

TABLE S4. Elastic constants of β and $\beta^{'}$-Te under different strains. The units of C_{ij} are N/m.

Monolayer	**Strain**	C_{11}	C_{12}	C_{13}	C_{16}	C_{22}	C_{23}	C_{26}	C_{33}	C_{36}	C_{66}
β-Te	Strain (0%)	13.52	6.69	-3.95	0.016	23.68	-2.52	0.026	-1.57	0.007	6.61
	Biaxial strain (4.5%)	15.98	2.70	0.048	-0.046	4.43	0.031	-0.024	0.086	-0.032	5.69
$\beta^{'}$-Te	Strain (0%)	16.42	2.01	-0.012	0.001	3.27	0.017	-0.002	0.05	-0.014	4.99
	biaxial strain (-5.5%)	13.08	6.75	0.054	0.034	23.01	0.029	-0.012	3.70	0.005	6.50
	uniaxial strain along zigzag(-4.9%)	11.57	1.39	0.035	0.030	13.57	0.014	0.005	1.90	0.008	6.45

TABLE S5. Elastic contants C_{11}, C_{22} and C_{12} of β-Te and $\beta^{'}$-Te in the units of GPa.

Monolayer	C_{11}	C_{22}	C_{12}
β-Te	7.95	13.93	3.93
$\beta^{'}$-Te	9.66	1.34	1.18

IX. PIEZOELECTRIC STRAIN COEFFICIENTS

Relation between piezoelectric stress and strain coefficients is

$$e_{ik} = \sum_{j}^{6} d_{ij} C_{jk} \tag{3}$$

We get four equations from this relation:

$$e_{21} = d_{21}C_{11} + d_{22}C_{12} + d_{23}C_{13} + d_{26}C_{16} \tag{4}$$

$$e_{22} = d_{21}C_{12} + d_{22}C_{22} + d_{23}C_{23} + d_{26}C_{26} \tag{5}$$

$$e_{23} = d_{21}C_{13} + d_{22}C_{23} + d_{23}C_{33} + d_{26}C_{36} \tag{6}$$

$$e_{26} = d_{21}C_{16} + d_{22}C_{26} + d_{23}C_{36} + d_{26}C_{66} \tag{7}$$

On solving these quations, we get the values of d_{21}, d_{22}, d_{23} and d_{26}, which have been given in Table 2.

X. GRÜNEISEN PARAMETERS

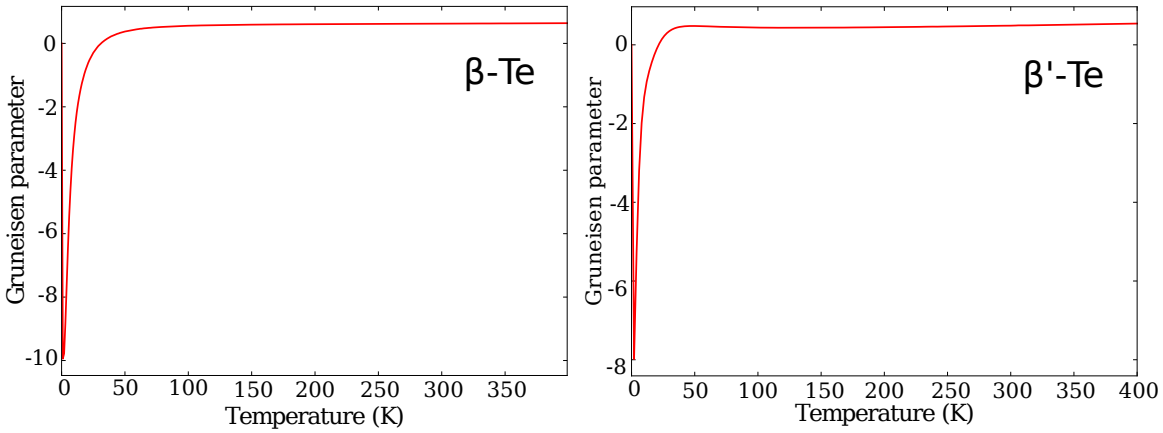

Figure S6. Variation of Grüneisen parameters of β-Te and $\beta^{'}$-Te with temperature.